Acta Crystallographica Section B
Structural Science
ISSN 0108-7681

Structures of *trans*-$[PtCl_2(PBz_3)_2]$, *trans*-$[PtI_2(PBz_3)_2]$, *trans*-$[Pt(NCS)_2(PBz_3)_2]\cdot 0.5C_6H_6$ and *trans*-$[PdI_2(PBz_3)_2]$

Maria H. Johansson,* Stefanus Otto† and Åke Oskarsson

Inorganic Chemistry 1, Centre for Chemistry and Chemical Engineering, Lund University, PO Box 124, S-221 00 Lund, Sweden

† On leave from Department of Chemistry, University of the Free State, Bloemfontein 9300, South Africa.

Correspondence e-mail: maria.johansson@inorg.lu.se

Received 29 September 2001
Accepted 12 December 2001

A series of structures of *trans*-$[MX_2(PBz_3)_2]$ [M = Pt, X = Cl^-; PBz_3 = tribenzylphosphine (1), I^-, *trans*-diiodobis(tribenzylphosphine)platinum(II) (2), and NCS^-, *trans*-di(thiocyanate)-bis(tribenzylphosphine)platinum(II) (3); M = Pd, X = I^-, *trans*-diiodobis(tribenzylphosphine)palladium(II) (4)] have been characterized by X-ray crystallography. In all compounds each tribenzylphosphine has one benzylcarbon close to the coordination plane. In (1), (2) and (4) those (in-plane) C atoms, from the two different PBz_3, exhibit an *anti* conformation along the P—P axis, while (3) has the *gauche* conformation. Root mean square (RMS) calculations and half-normal probability plots show that the complexes in (2) and (4) are very similar and the only significant differences between them are the M—P bonds, 2.354 (4) and 2.330 (5) Å, and the M—I bond distances, 2.604 (1) and 2.611 (2) Å, for Pd and Pt, respectively. Calculations of the steric demand of the PBz_3 ligands based on the Tolman model gave values ranging from 155 to 178° for the effective and 156 to 179° for the Tolman angles, respectively.

1. Introduction

We have recently shown how different packing arrangements can be induced in crystal structures of *trans*-$[PtCl_2(AsPh_3)_2]$ by co-crystallizing the metal complex with different solvent molecules (Johansson *et al.*, 2000). One intriguing observation from the *trans*-$[PtCl_2(AsPh_3)_2]$ study was the similarity of the torsion angles around the Pt—As bonds in all four structures investigated. Each of the triphenylarsine ligands has one As—C bond close to the coordination plane, the Cl—Pt—As—C torsion angles range between −12.6 (1) and −17.8 (1)°, with one outlier at −25.8 (1)°. The same orientation was also found for *trans*-$[PtCl_2(PPh_3)_2]$ and other closely related structures (Johansson & Otto, 2000). One crystal structure of a mononuclear platinum(II) complex containing two tribenzylphosphines, *trans*-$[PtH(OPh)(PBz_3)_2]$ (Seligson *et al.*, 1991), and two palladium(II) complexes, *trans*-$[PdX_2(PBz_3)_2]$ (X = N_3^- and CN^-; Bendiksen *et al.*, 1982), have been reported previously in the literature. In both of the reported palladium structures the rotation of the PBz_3 ligands were similar to those encountered in the arsine structures, *i.e.* one of the benzylcarbons lie almost in the coordination plane, with torsion angles, X—Pd—P—C −12.2 and −18.6°, respectively.

We have now extended this study by varying the X ligand as well as the metal in a series of *trans*-$[MX_2(PBz_3)_2]$ [M = Pt, X = Cl^- (1), I^- (2) and NCS^- (3); M = Pd, X = I^- (4); PBz_3 = tribenzylphosphine] complexes. Due to the CH_2 spacers between the P atom and the Ph rings in the PBz_3 ligand, a larger flexibility compared with PPh_3 is possible.

Table 1
Experimental details.

	(1)	(2)	(3)	(4)
Crystal data				
Chemical formula	$[PtCl_2(PBz_3)_2]$	$[PtI_2(PBz_3)_2]$	$[Pt(NCS)_2(PBz_3)_2]$	$[PdI_2(PBz_3)_2]$
Chemical formula weight	874.69	1057.59	959	968.9
Cell setting, space group	Triclinic, $P\overline{1}$	Monoclinic, Pn	Triclinic, $P\overline{1}$	Monoclinic, Pn
a, b, c (Å)	9.4657 (19), 10.609 (2), 19.018 (4)	11.256 (2), 9.985 (2), 18.126 (4)	9.5006 (19), 11.800 (2), 19.112 (4)	11.274 (2), 9.994 (2), 18.073 (4)
α, β, γ (°)	82.50 (3), 82.75 (3), 88.59 (3)	90, 105.05 (3), 90	83.99 (3), 89.87 (3), 81.98 (3)	90, 104.88 (3), 90
V (Å^3)	1878.2 (6)	1967.3 (7)	2109.7 (7)	1968.1 (7)
Z	2	2	2	2
D_x (Mg m^{-3})	1.547	1.785	1.510	1.635
Radiation type	Mo $K\alpha$	Mo $K\alpha$	Mo $K\alpha$	Mo $K\alpha$
No. of reflections for cell parameters	8192	6340	4783	3723
θ range (°)	2.5–29	2.4–26.2	2.4–22.6	2.3–23.4
μ (mm^{-1})	3.992	5.245	3.535	2.149
Temperature (K)	293 (2)	293 (2)	293 (2)	293 (2)
Crystal form, colour	Rectangle, yellow	Prism, orange	Prism, white	Rectangle, red
Crystal size (mm)	0.20 × 0.15 × 0.08	0.30 × 0.07 × 0.06	0.30 × 0.06 × 0.05	0.40 × 0.20 × 0.08
Data collection				
Diffractometer	Bruker SMART CCD	Bruker SMART CCD	Bruker SMART CCD	Bruker SMART CCD
Data collection method	ω scans	ω scans	ω scans	ω scans
Absorption correction	Empirical	Empirical	Empirical	Empirical
T_{min}	0.428	0.427	0.529	0.398
T_{max}	0.622	0.605	0.736	0.698
No. of measured, independent and observed parameters	20 587, 11 405, 8135	20 794, 10 810, 7389	21 262, 11 257, 6396	17 698, 8765, 4496
Criterion for observed reflections	$I > 2\sigma(I)$	$I > 2\sigma(I)$	$I > 2\sigma(I)$	$I > 2\sigma(I)$
R_{int}	0.0259	0.0510	0.0528	0.0920
θ_{max} (°)	31.92	31.54	29.13	29.13
Range of h, k, l	$-13 \rightarrow h \rightarrow 13$ $-15 \rightarrow k \rightarrow 13$ $-26 \rightarrow l \rightarrow 28$	$-16 \rightarrow h \rightarrow 15$ $-14 \rightarrow k \rightarrow 14$ $-23 \rightarrow l \rightarrow 26$	$-12 \rightarrow h \rightarrow 13$ $-13 \rightarrow k \rightarrow 16$ $-26 \rightarrow l \rightarrow 26$	$-15 \rightarrow h \rightarrow 15$ $-13 \rightarrow k \rightarrow 13$ $-24 \rightarrow l \rightarrow 22$
Refinement				
Refinement on	F^2	F^2	F^2	F^2
$R[F^2>2\sigma(F^2)]$, $wR(F^2)$, S	0.0311, 0.0796, 1.005	0.0356, 0.0706, 0.9	0.0425, 0.0868, 0.868	0.0511, 0.1249, 0.852
No. of reflections and parameters used in refinement	11 405, 427	10 810, 425	11 257, 487	8765, 424
H-atom treatment	H, riding model	H, riding model	H, riding model	H, riding model
Weighting scheme	$w = 1/[\sigma^2(F_o^2) + (0.0395P)^2 + 0.5874P]$, where $P = (F_o^2 + 2F_c^2)/3$	$w = 1/[\sigma^2(F_o^2) + (0.0271P)^2]$, where $P = (F_o^2 + 2F_c^2)/3$	$w = 1/[\sigma^2(F_o^2) + (0.0310P)^2]$, where $P = (F_o^2 + 2F_c^2)/3$	$w = 1/[\sigma^2(F_o^2) + (0.0576P)^2]$, where $P = (F_o^2 + 2F_c^2)/3$
$(\Delta/\sigma)_{max}$	0.001	0.001	0.000	0.000
$\Delta\rho_{max}$, $\Delta\rho_{min}$ (e Å^{-3})	0.862, −1.486	1.034, −0.975	0.75, −0.946	0.577, −0.843

Except for electronic properties, the size of a ligand is of additional importance in determining its coordination behaviour to a metal centre. The most widely recognized expression of the size of phosphine and related ligands is the Tolman cone angle (Tolman, 1977). It has been observed earlier that flexible ligands may adopt various spatial conformations resulting in very different values obtained from their cone-angle calculations (Ferguson *et al.*, 1978).

2. Experimental

All NMR spectra were recorded in $CDCl_3$ at 293 K on a Varian Unity 300 spectrometer operating at 299.78, 121.35 and 64.17 MHz for the ^{1}H, ^{31}P and ^{195}Pt nuclei, respectively. The ^{1}H spectra were referenced relative to the residual $CHCl_3$ peak (7.25 p.p.m.), the ^{31}P spectra relative to an external standard of 85% H_3PO_4 (0 p.p.m.) and the ^{195}Pt spectra relative to an external standard of H_2PtCl_6 (1 g of H_2PtCl_6 in 3 ml of 1 *M* HCl containing 50% D_2O, 0 p.p.m.). In all cases positive shifts are downfield and coupling constants are in Hz.

2.1. Synthesis

The starting materials $[PtCl_2(SMe_2)_2]$ and $[PdCl_2(SMe_2)_2]$ were prepared according to literature methods (Byers *et al.*, 1998; Hill *et al.*, 1998), while PBz_3 was purchased from Aldrich and used as received. All preparations were carried out under aerobic conditions using reagent-grade solvents.

Table 2
Selected NMR parameters.

Complex	δ (CH_2) (p.p.m.)	δ (P) (p.p.m.)	δ (Pt) (p.p.m.)	$^1J_{Pt-P}$ (Hz)
trans-[$PtCl_2(PBz_3)_2$]	3.38	6.72	−3957	2460
trans-[$PtI_2(PBz_3)_2$]	3.80	−8.87	−5470	2338
trans-[$Pt(NCS)_2(PBz_3)_2$]	3.27	10.66	−3777	2302
trans-[$PdI_2(PBz_3)_2$]	3.79	0.49		

2.1.1. *trans*-[$PtCl_2(PBz_3)_2$] (1). PBz_3 (90 mg, 0.296 mmol) was added to an acetone (10 ml) solution of *cis*/*trans*-[$PtCl_2(SMe_2)_2$] (50 mg, 0.128 mmol). The mixture was stirred for 1 h, which facilitated the precipitation of the desired product in almost quantitative yield. The crude product was collected by filtration and recrystallization from chloroform gave light yellow crystals suitable for X-ray analysis.

2.1.2. *trans*-[$PtI_2(PBz_3)_2$] (2). Bu_4NI (125 mg, 0.338 mmol) was added to a dichloromethane (10 ml) solution of *trans*-[$PtCl_2(PBz_3)_2$] (30 mg, 0.343 mmol) and was stirred for 1 h. The reaction mixture was evaporated to dryness and the residues washed with methanol to remove excess Bu_4NI and the Bu_4NCl formed during the reaction. Recrystallization from chloroform gave dark yellow crystals suitable for X-ray analysis.

2.1.3. *trans*-[$Pt(NCS)_2PBz_3)_2$] (3). The same general procedure was used as described for (2), but using Bu_4NSCN (105 mg, 0.349 mmol) during the preparation. Recrystallization from a mixture of dichloromethane and benzene gave white crystals suitable for X-ray analysis.

2.1.4. *trans*-[$PdI_2(PBz_3)_2$] (4). The same general procedure was used as described for (1) and (2). Recrystallization from a mixture of dichloromethane and acetone gave red crystals suitable for X-ray analysis.

2.2. Crystallography and calculations

Crystal data and details about the data collections and refinements are given in Table 1.[1] All intensity data sets were collected at 293 (1) K with a Bruker SMART CCD system using ω scans and a rotating anode with Mo $K\alpha$ radiation (λ = 0.71073 Å; Bruker AXS, 1995*b*). The first 50 frames were recollected at the end of each data collection to check for decay; no decay was observed for any of the structures. All reflections were merged and integrated using *SAINT* (Bruker AXS, 1995*a*) and the intensities were corrected for Lorentz, polarization and absorption effects using *SADABS* (Sheldrick, 1996). Structures (1), (2) and (3) were solved by direct methods, while (4) was solved by Patterson methods. All structures were refined by full-matrix least-squares calculations on F^2 using *SHELXTL*5.1 (Sheldrick, 1997*b*). All non-H atoms were refined with anisotropic displacement parameters, while the H atoms were constrained to parent sites, using a riding model. No high residual electron densities (>1.5 e^- Å^{-3}) were found in the final difference Fourier maps for any of the structures.

All structures were checked for solvent-accessible cavities and the percentage of filled space was calculated using *PLATON* (Spek, 1990), the graphics were created with *DIAMOND* (Brandenburg, 1997), RMS calculations and overlay plots were made with *SHELXP*5.1 (Sheldrick, 1997*a*) and the half-normal probability plots with *EXCEL*2000.

The cone-angle calculations are based on Tolman's model (Tolman, 1977) using C—H bond distances of 0.93 Å for the aromatic C atoms and 0.96 Å for CH_2 and a van der Waals radius of hydrogen of 1.2 Å. The effective cone angle is calculated in a similar way as the Tolman cone angle, but by using the actual Pt—P bond distance as determined from the crystallography, while a fixed distance, 2.28 Å, is used for the Tolman cone-angle calculations.

3. Results and discussion

3.1. NMR characterization

A summary of the most important NMR parameters is given in Table 2. A single resonance in the ^{31}P NMR spectrum suggests the phosphine ligands to be chemically equivalent and the $^1J_{PtH}$ coupling constants indicate a *trans* configuration with respect to each other. During the preparation and isolation of the various complexes no indication of any *cis* isomers was found. From the ^1H NMR data it can be seen that the CH_2 group of the phosphine ligands are quite sensitive to the nature of the metal centre and show a trend of lower chemical shifts for the heavier atoms, similar to that observed for the chemical shifts of the P atoms. The presence of the benzene solvent molecule in (3) was verified by dissolving crystals, from the same batch as used for the X-ray data collection, in $CDCl_3$ and recording the ^1H NMR spectrum. A

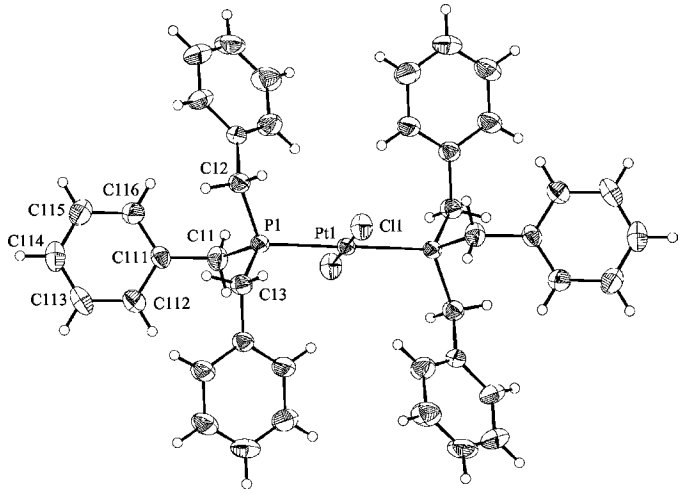

Figure 1
Numbering scheme for (1). Thermal ellipsoids at 30% probability.

[1] Supplementary data for this paper are available from the IUCr electronic archives (Reference: NS0007). Services for accessing these data are described at the back of the journal.

Table 3
Selected bond distances (Å), bond angles (°), torsion angles (°) and calculated cone angles (°), the effective θ_E and Tolmans θ_T.

	(1) part 1	(1) part 2	(2)	(3)	(4)
M—P1	2.3219 (12)	2.3019 (10)	2.3262 (19)	2.3197 (14)	2.351 (3)
M—P2			2.333 (2)	2.3244 (14)	2.356 (3)
M—*X*1	2.3092 (11)	2.3053 (10)	2.6122 (9)	1.966 (5)	2.6045 (12)
M—*X*2			2.6099 (9)	2.014 (5)	2.6030 (12)
P1—C11	1.828 (4)	1.829 (3)	1.835 (7)	1.817 (5)	1.840 (10)
P1—C12	1.837 (4)	1.831 (3)	1.826 (7)	1.831 (5)	1.832 (11)
P1—C13	1.838 (4)	1.835 (3)	1.848 (7)	1.812 (5)	1.843 (10)
P2—C21			1.846 (8)	1.818 (5)	1.845 (11)
P2—C22			1.825 (7)	1.822 (5)	1.834 (12)
P2—C23			1.825 (7)	1.826 (5)	1.842 (10)
N—C				1.139 (6)	
				1.058 (6)	
C—S				1.602 (6)	
				1.666 (7)	
P1—*M*—P2	180.0	180.0	179.86 (9)	172.40 (5)	179.94 (14)
*X*1—*M*—*X*2	180.0	180.0	179.81 (2)	176.97 (19)	179.50 (5)
P1—*M*—*X*1	92.93 (4)	92.784	92.74 (5)	91.84 (12)	92.65 (7)
P1—*M*—*X*2	87.07 (4)	87.224	87.19 (5)	88.32 (12)	87.23 (7)
P2—*M*—*X*1			87.15 (5)	90.79 (12)	87.32 (7)
P2—*M*—*X*2			92.92 (5)	89.44 (12)	92.80 (7)
M—P1—C11	114.66 (12)	113.50 (12)	116.9 (2)	112.72 (17)	117.2 (4)
M—P1—C12	114.11 (12)	114.46 (12)	114.1 (3)	116.72 (18)	113.8 (4)
M—P1—C13	114.44 (13)	115.61 (11)	115.6 (3)	108.41 (17)	115.8 (4)
M—P2—C21			116.6 (2)	117.80 (18)	117.1 (4)
M—P2—C22			114.0 (3)	109.97 (17)	113.9 (4)
M—P2—C23			115.9 (3)	112.25 (18)	115.6 (3)
C11—P1—C12	107.06 (19)	107.99 (16)	104.4 (4)	109.1 (3)	103.5 (5)
C12—P1—C13	97.14 (17)	97.68 (15)	97.5 (3)	100.9 (2)	96.8 (5)
C11—P1—C13	107.81 (19)	105.82 (17)	106.0 (4)	108.1 (2)	107.2 (5)
C21—P2—C22			104.3 (4)	107.0 (2)	104.2 (5)
C22—P2—C23			97.3 (3)	105.6 (2)	97.4 (5)
C21—P2—C23			106.5 (4)	103.3 (2)	106.4 (5)
*X*1—Pt—P1—C11	1.6 (2)	1.08 (15)	2.1 (3)	0.8 (2)	0.8 (4)
*X*1—Pt—P1—C12	−123.44 (14)	−121.47 (12)	−120.1 (3)	−128.2 (2)	−120.1 (3)
*X*1—Pt—P1—C13	125.89 (14)	127.56 (12)	128.0 (3)	118.7 (2)	129.0 (4)
*X*1—Pt—P2—C21			−175.9 (3)	−15.2 (2)	176.5 (4)
*X*1—Pt—P2—C22			62.4 (3)	104.6 (2)	−61.7 (4)
*X*1—Pt—P2—C23			−49.4 (2)	−138.2 (2)	49.9 (4)
θ_E	162	160	155	178	155
			161	165	162
θ_T	164	160	156	179	157
			163	167	164

singlet at 7.36 p.p.m. was found and integrated to the correct ratio. In the ^{195}Pt NMR spectrum of (3) splitting due to nitrogen with a coupling constant of 443 Hz is noticed, suggesting a first-order ^{195}Pt–^{14}N interaction and hence N coordinated thiocyanate ligands. This coupling constant is in the same range as for *trans*-[Pt(NCS)$_2$(PEt$_3$)$_2$] (Anderson *et al.*, 1976; Pregosin, 1982). The ^{1}H spectra of (2) and (4) are basically identical, while the ^{31}P chemical shifts differ by 9.36 p.p.m. with the P in the Pd complex resonating at lower field with respect to that in the Pt complex, indicating less electron density on the phosphorus in the palladium complex.

3.2. Description of the structures

The numbering schemes with thermal ellipsoids for (1) and (2) are given in Figs. 1 and 2. A summary of selected geometrical parameters is given in Table 3. All four compounds have distorted square planar geometries around the central metal atom with the tribenzylphosphine ligands in a *trans* orientation.

In (1), *trans*-[PtCl$_2$(PBz$_3$)$_2$], which crystallizes in the triclinic space group $P\overline{1}$, there are two independent half molecules, with Pt atoms on inversion centres (Fig. 3). The main difference between the two molecules is in the orientation of the phenyl rings, as shown in Fig. 4. The two platinum coordination planes have an angle of 124.7° with respect to one another. At a distance of 2.94 Å, H132 is in an approximate axial position to Pt1 and similarly H226 has a distance of 2.97 Å to Pt2. No classical intermolecular hydrogen bonds are found and 67% of the space in the unit cell is filled.

trans-[PtI$_2$(PBz$_3$)$_2$] (2) crystallizes in the monoclinic space group *Pn*. The $|E^*E - 1|$ value of 0.700 indicates a non-centrosymmetric space group as well as twinning. The absolute structural parameter refined to 0.449 (5) (Flack, 1983) and the structure was subsequently refined as a racemic twin. H126 and H226 are positioned 2.99 and 2.85 Å from the platinum, respectively, one on each side of the coordination plane. No classical intermolecular hydrogen bonds are found and the space in the unit cell is filled to 66%.

In (3), *trans*-[Pt(NCS)$_2$(PBz$_3$)$_2$]·0.5C$_6$H$_6$, which crystallizes in the triclinic space group

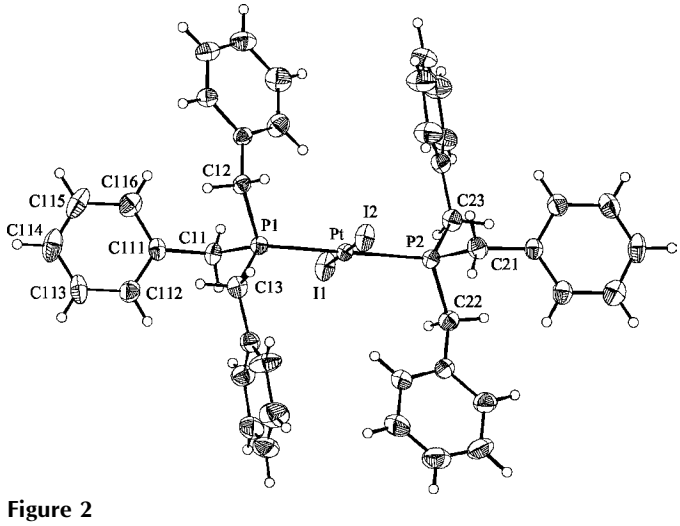

Figure 2
Numbering scheme for (2). Thermal ellipsoids at 30% probability.

$P\bar{1}$, $Z = 2$, the Pt atom is in a general position. Each unit cell contains a single benzene solvent molecule, which lies on the inversion centre at $0,\frac{1}{2},\frac{1}{2}$. The NCS groups are close to linear, 178.92 (5) and 177.83 (6)° for N1—C1—S1 and N2—C2—S2, respectively. No classical intermolecular hydrogen bonds are found and no H atoms are within 3 Å of the Pt or the S atoms. The unit cell is filled to 63% by the platinum complexes and to 67% when the solvent is included.

Compound (4), *trans*-$[PdI_2(PBz_3)_2]$, is isostructural to its platinum analogue (2). The $|E^*E - 1|$ value is 0.768, also indicative of a non-centrosymmetric space group. The absolute structure parameter refined to 0.08 (3), indicating an almost single crystal. H226 and H126 are positioned at 2.84 and 2.95 Å from the Pd atom, one on each side of the coordination plane. No classical intermolecular hydrogen bonds were found and the space in the unit cell is filled to 66%. An overlay plot of (2) and (4) is shown in Fig. 5. RMS calculation, using (2) and (4), with all non-H atoms gives a value of 0.0325 Å, representing the best fit for two individual structures in this study.

In all four structures each PBz_3 ligand has one X—Pt—P—C torsion angle close to 0 or 180°, showing that one of the benzylcarbons is close to the coordination plane. The largest deviation is observed for one of the ligands in (3) with a deviation of 15.2 (2)°; the others do not deviate by more than 5°. However, there is an interesting dissimilarity of the orientation of the benzylcarbons. In (1), (2) and (4) the two benzylcarbons in the coordination plane (C11 and C21) are *anti* along the P—P axis, implying a psuedo-inversion centre in the complex, while in (3) they are *gauche* (Fig. 6). This preferable orientation may be indicative of a conformational energy minimum in rotation around the Pt—P bond, probably where the most sufficient orbital overlap is experienced between the filled *d*-orbitals of the metal and the LUMO (mixture of *d* and σ^* orbitals) of the phosphine and arsine ligands (Dunne *et al.*, 1991). Extended Hückel calculations using the program *CACAO* (Maelli & Proserpio, 1990) indicate that there are energy minima for both conformations. However, the difference between the *anti* and *gauche* conformations along the P—P axis seems to be marginal. Although a slightly lower energy minimum was obtained for the *gauche* conformation in (3), its unusual geometry may be due to packing effects.

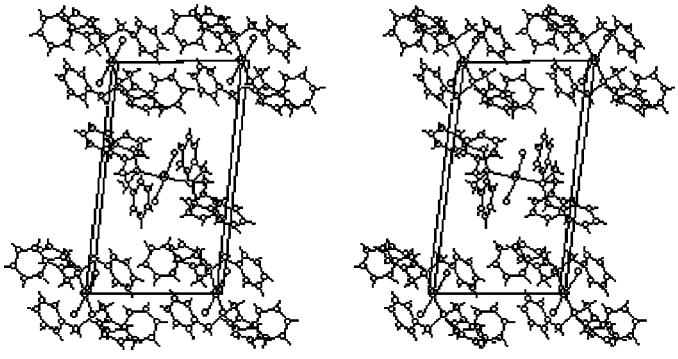

Figure 3
Packing diagram for (1).

3.3. Cone-angle calculations

The values for the effective (θ_E) and Tolman (θ_T) cone angles for the PBz_3 ligands are listed in Table 3. The flexibility of the PBz_3 ligand is clearly illustrated by the large variation in cone angles encountered with the effective values (using the experimental M—P bond distances) ranging from 155 to 178°, with an average value of 162°. Due to the fact that the actual bond distances are all slightly longer than the 2.28 Å used to calculate the Tolman cone angles these are marginally larger

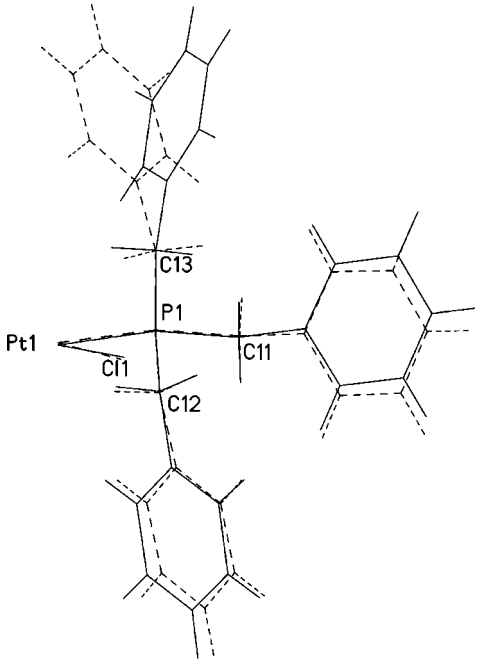

Figure 4
Overlay plot of parts 1 and 2 (dashed line) of complex (1).

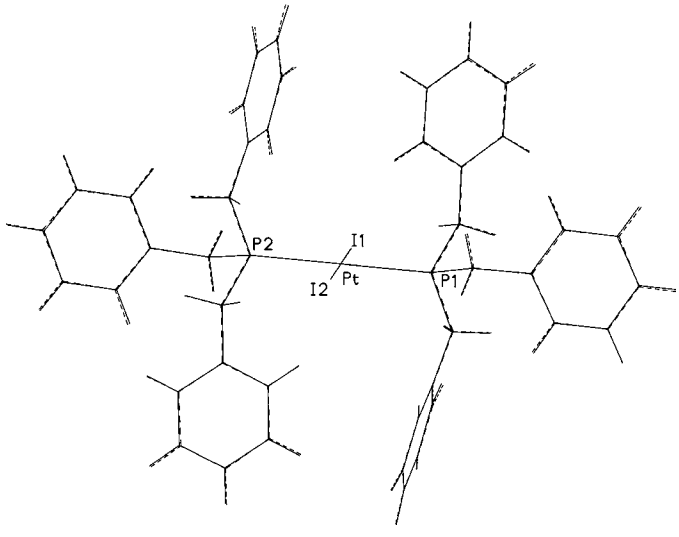

Figure 5
Overlay plot of (2) and (4) (dashed line).

Table 4
Most divergent δm_i values for the corresponding interatomic distances for the complexes compared in Fig. 7(*b*).

First-, second- and third-order numbers represent the closest distance between two atoms separated by one, two and three formal bonds.

From Fig. 7(*b*) [(2) *versus* (4)]		
δm_i	Distance	Order No.
12.77	P1—P2	2
7.57	Pt/Pd—P1	1
6.70	Pt/Pd—P2	1
6.25	I1—I2	2
5.13	Pt/Pd—I1	1
4.6	Pt/Pd—I2	1

in all cases, ranging from 156 to 179°, with an average of 164°. These average values are all in excellent agreement with the value of 165° proposed by Tolman in his original work (Tolman, 1977). It is however significantly smaller than the 200° and 232° reported previously for $PdX_2(PBz_3)_2$ (X^- = N_3 and CN; Bendiksen *et al.*, 1982). The current study indicates that 165 ± 12° may be a more reasonable estimation for these cone angles.

3.4. Half-normal probability plots

Half-normal probability plots are used to estimate the reliability of the s.u.'s and to identify systematic geometric differences in two molecules (Abrahams & Keve, 1971; De Camp, 1973). Random errors of differences in interatomic distances are approximately normally distributed (Albertsson & Schultheiss, 1974). Observed values of δm_i calculated using (1) are plotted *versus* the values α_i expected for a half-normal distribution of errors (International Tables for X-ray Crystallography, 1974, Vol. IV).

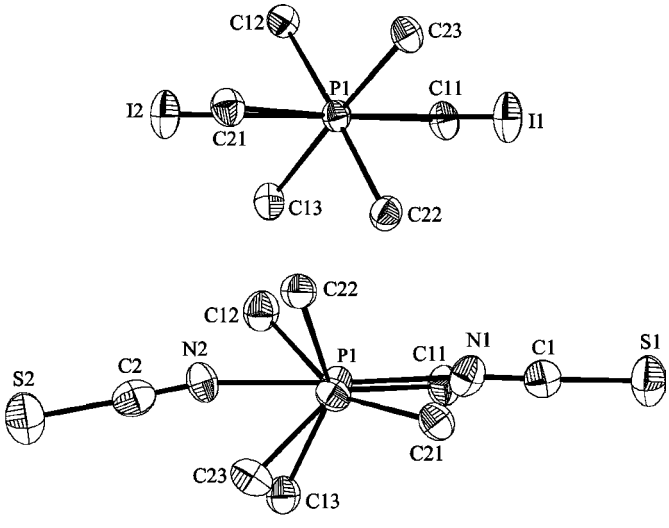

Figure 6
View of (2) and (3) along the P—Pt—P bond showing the *anti* conformation (C11—P1—P2—C21 ≃ 180°) for (2) and the *gauche* conformation (C11—P1—P2—C21 ≃ 0°) for (3).

$$\delta m_i = \frac{\left|d(1)_i - d(2)_i\right|}{\left[\sigma^2 d(1)_i + \sigma^2 d(2)_i\right]^{1/2}}. \qquad (1)$$

The quantities $d(1)_i$ and $d(2)_i$ are interatomic distances for two different structures (1) and (2) with s.u.'s $\sigma d(1)_i$ and $\sigma d(2)_i$, respectively. Two types of comparisons can be made, one with independent distances and a second one with dependent distances (representing atoms separated by one, two or three formal bonds). From the first comparison the slope gives an indication of the reliability of the s.u.'s, *i.e.* if the slope is larger or smaller than 1, the s.u.'s are under- or overestimated, respectively, and from the second comparison it is possible to identify major systematic differences between the two structures.

Half-normal probability analysis including all 47 non-H atoms has been made on the two isostructural complexes (2) and (4), with 135 independent interatomic distances ($3n - 6$) completely describing the complex. Fig. 7(*a*), based on the independent distances, gives a straight line for the first 131 distances with a slope of 1.633 ± 0.025 showing the s.u.'s to be underestimated only by a factor of 1.6. The intercept 0.034 ± 0.023 indicates that only negligible systematic experimental differences are present. The most divergent δm_i values, obtained from Fig. 7(*b*) (dependent distances), are listed in Table 4. The only significant differences between the two complexes are the lengthening of the *M*—P and the shortening of the *M*—I distances for palladium compared with platinum.

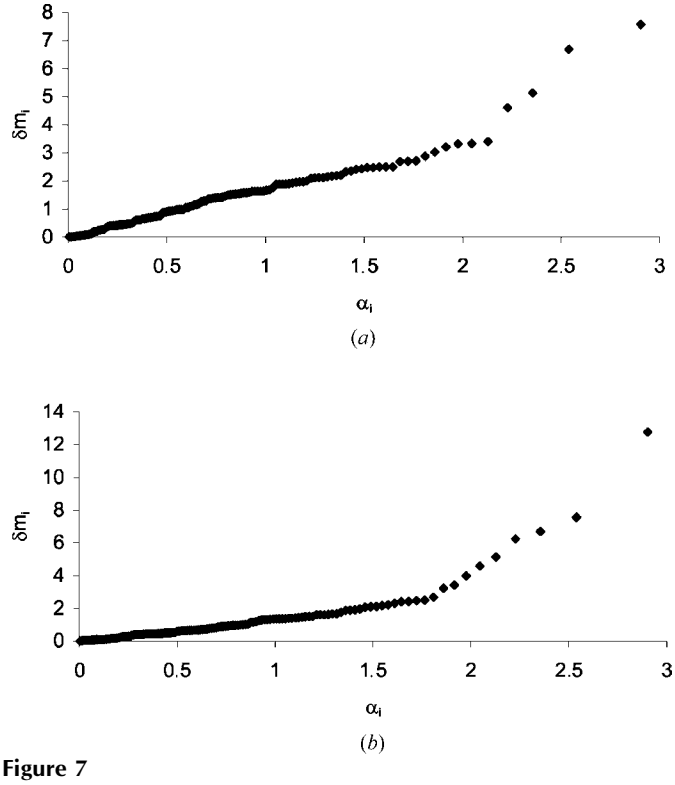

Figure 7
Half-normal probability plots based on 135 distances for (2) *versus* (4). (*a*) Independent distances. The least-squares fit, based on the first 131 distances, gives a slope of 1.633 ± 0.025 and intercept 0.034 ± 0.023, correlation coefficient 0.992. The errors indicate a 95% confidence interval. (*b*) Dependent distances.

In conclusion, all tribenzylphosphines have one benzyl-carbon close to the coordination plane and in structures (1), (2) and (4) these C atoms are *anti* along the P—P axis, while in (3) they are *gauche*. Cone-angle calculations confirmed the flexible nature of the PBz_3 ligands. Individual values range from 155 to 178° and 156 to 179° for the effective and Tolman cone angles, respectively, with averages of 162 and 164°. The only significant differences between the two isostructural iodo complexes, (2) and (4), are the lengthening of the *M*—P bonds and the shortening of the *M*—I bond distances for palladium compared with platinum (Table 3).

Financial support from the Swedish Natural Science Research Council, Crafoord Foundation, Swedish International Development Cooperation Agency (grant holder: Professor L. I. Elding), the South African NRF and the Research Fund of the University of the Free State are gratefully acknowledged.

References

Abrahams, S. C. & Keve, E. T. (1971). *Acta Cryst.* A**27**, 157–165.
Albertsson, J. & Schultheiss, P. M. (1974). *Acta Cryst.* A**30**, 854–855.
Anderson, S. J., Goggin, P. L. & Goodfellow, R. J. (1976). *J. Chem. Soc. Dalton Trans.* pp. 1959–1964.
Bendiksen, B., Riley, W. C., Babich, M. W., Nelson, J. H. & Jacobson, R. A. (1982). *Inorg. Chim. Acta*, **57**, 29–36.
Brandenburg, K. (1997). *DIAMOND Crystal Impact.* Bonn, Germany.
Bruker AXS (1995*a*). *SAINT Integration Software.* Bruker Analytical X-ray System, Madison, Wisconsin, USA.
Bruker AXS (1995*b*). *SMART Area Detector Control Software.* Bruker Analytical X-ray System, Madison, Wisconsin, USA.
Byers, P. K., Canty, A. J., Jin, H., Kruis, D., Markies, B. A., Boersma, J. & van Koten, G. (1998). *Inorg. Synth.* **32**, 163–164.
De Camp, W. H. (1973). *Acta Cryst.* A**29**, 148–150.
Dunne, B. J., Morris, R. B. & Orpen, A. G. (1991). *J. Chem. Soc. Dalton Trans.* pp. 653–661.
Ferguson, G., Roberts, P. J., Alyea, E. C. & Khan, M. (1978). *Inorg. Chem.* **17**, 2965–2967.
Flack, H. D. (1983). *Acta Cryst.* A**39**, 876–881.
Hill, G. S., Irwin, M. J., Levy, C. J., Rendina, L. M. & Puddephatt, R. J. (1998). *Inorg. Synth.* **32**, 149–150.
Johansson, M. H. & Otto, S. (2000). *Acta Cryst.* C**56**, e12–e15.
Johansson, M. H., Otto, S., Roodt, A. & Oskarsson, Å. (2000). *Acta Cryst.* B**56**, 226–233.
Maelli, C. & Proserpio, D. M. (1990). *J. Chem. Educ.* **67**, 399–402.
Pregosin, P. S. (1982). *Coord. Chem. Rev.* **44**, 247–290.
Seligson, A. L., Cowan, R. L. & Trogler, W. C. (1991). *Inorg. Chem.* **30**, 3371–3381.
Sheldrick, G. M. (1996). *SADABS.* University of Göttingen, Germany.
Sheldrick, G. M. (1997*a*). *SHELXP*5.1. University of Göttingen, Germany.
Sheldrick, G. M. (1997*b*). *SHELXTL*5.1. University of Göttingen, Germany.
Spek, A. L. (1990). *Acta Cryst.* A**46**, C-34.
Tolman, C. A. (1977). *Chem. Rev.* **77**, 313–348.